Fuel 93 (2012) 567–575

Contents lists available at SciVerse ScienceDirect

Fuel

journal homepage: www.elsevier.com/locate/fuel

Effects of pyrolysis conditions on the heating rate in biomass particles and applicability of TGA kinetic parameters in particle thermal conversion modelling

Ramin Mehrabian [a,b,*], Robert Scharler [a,b,c], Ingwald Obernberger [a,b,c]

[a] BIOENERGY 2020+ GmbH, Inffeldgasse 21b, 8010 Graz, Austria
[b] Institute for Process and Particle Engineering, Graz University of Technology, Inffeldgasse 21b, 8010 Graz, Austria
[c] BIOS BIOENERGIESYSTEME GmbH, Inffeldgasse 21b, 8010 Graz, Austria

ARTICLE INFO

Article history:
Received 14 January 2011
Received in revised form 30 June 2011
Accepted 27 September 2011
Available online 12 October 2011

Keywords:
Biomass
Pyrolysis
TGA
Heating rate

ABSTRACT

A one-dimensional single particle model is utilised to investigate the effects of radiation temperature, moisture content, particle size and biomass physical properties on the heating rate in biomass particles during pyrolysis. The model divides the particle into four layers – drying, pyrolysis, char and ash layer – corresponding to the four main stages of biomass thermal conversion. The average of the time derivative of the pyrolysis layer centre temperature weighted by the pyrolysis rate is introduced as an appropriate indicator for the heating rate in the particle during pyrolysis. The influencing parameters on the heating rate are summarised in the Biot number and the thermal time constant, to make the investigation of their effects easier. The heating rate is inversely proportional to the thermal time constant. The effect of a variation of the Biot number on the heating rate is negligible in comparison to the thermal time constant. Therefore, the thermal time constant can be sufficiently used to specify the heating rate regimes during pyrolysis. It is found that for thermal time constants of more than 50 s, pyrolysis takes place in a low heating rate regime, i.e. less than 50 K/min. Additionally, the heating rate during pyrolysis of various biomass types under a wide range of thermal conversion conditions has been examined, in order to classify the heating rate regime of pyrolysis in state-of-the-are combustion/gasification plants. The pyrolysis of wood dust and wood pellets is found to happen always in high heating rate regimes. Therefore, the kinetic parameters obtained by conventional TGA systems (typically with heating rates lower than 50 K/min) are not applicable for them. On the contrary, the pyrolysis of wood logs always happens in low heating rate regimes, which indicates that kinetic parameters obtained by conventional TGA systems can be applied. However, pyrolysis of wood chips can undergo low or high heating rate regimes depending on their particle size. Concerning the moisture content, it can be stated that it does not strongly influence the heating rate regime of certain biomass particles.

1. Introduction

Due to the importance of modelling the thermal conversion of biomass particles for the design and optimisation of biomass combustion systems, several studies have been performed to describe the thermo-chemical conversion of biomass fuels [1–9]. Since, a combination of several sub-processes such as heat-up, drying, pyrolysis, and char burnout represents the global process of thermal conversion of solid biomass particles, all the presented models include a sub-model for pyrolysis. Usually the rate of biomass pyrolysis is described by an Arrhenius equation. The results of TGA experiments are used to determine the empirical constants of the Arrhenius equation.

Most of the TGA experiments have been performed under low heating rate conditions, e.g. less than 50 K/min, because high heating rate TGA measurements are rather complex. However, it is known that heating rates of the TGA experiments influence the characteristics of thermogravimetric curves [10–13]. Indeed, the pyrolysis rate is affected by the heating rate in the particle and it leads to different kinetic parameters. Therefore, it is crucial to know under which conditions pyrolysis occurs in low/high heating rate regimes, in order to apply the appropriate TGA kinetic parameters.

In this paper, a numerical model for the thermal conversion of thermally thick particles has been used to study the influence of different parameters on the heating rate during pyrolysis. The influencing parameters on the heating rate are summarised in

* Corresponding author at: BIOENERGY 2020+ GmbH, Inffeldgasse 21b, 8010 Graz, Austria. Tel.: +43 (0) 316 8739232; fax: +43 (0) 316 8739202.
E-mail address: ramin.mehrabian@bioenergy2020.eu (R. Mehrabian).

0016-2361/$ - see front matter © 2011 Elsevier Ltd. All rights reserved.
doi:10.1016/j.fuel.2011.09.054

Nomenclature

A	pre-exponential factor (s^{-1})
Bi	Biot number (–)
c_i	biomass pseudo-component contributions (–)
c_p	specific heat capacity (J kg^{-1} K^{-1})
D	diameter (m)
$\mathcal{D}$	diffusivity (m^2 s^{-1})
E	activation energy (kJ mol^{-1})
h	heat transfer coefficient (W m^{-2} K^{-2})
h_m	mass transfer coefficient (m s^{-1})
k	kinetic rate constant (s^{-1})
L_c	characteristic length scale (m)
m	mass (kg)
M_c	carbon molecular weight (kg $kmol^{-1}$)
MC	moisture content, wet based (%)
Nu	Nusselt number (–)
R	universal gas constant (kJ mol^{-1} K^{-1})
S	surface area (m^2)
t	time (s)
T	temperature (K)
T_m	temperature at maximum conversion rate (K)
X_∞	molar concentration of gas species at bulk flow (mol m^{-3})

Greek symbols

α_i	conversion of each biomass pseudo-component (–)
β	heating rate (K s^{-1})
δ_{ash}	thickness of ash layer (m)
ϵ	emissivity (–)
ϕ	porosity (–)
η	tortuosity (–)
λ	thermal conductivity (W m^{-1} K^{-1})
ρ	density (kg m^{-3})
σ	Stefan–Boltzmann constant (W m^{-2} K^{-4})
τ	thermal time constant (s)
Ω	stoichiometric ratio of moles of carbon per mole of oxidising/gasifying agent in corresponding reaction (–)

Subscripts

0	initial condition
conv	convection
e	effective
f	final condition
g	gas
p	particle
pl	pyrolysis layer
rad	radiation
s	solid

two characteristic numbers, the Biot number and the thermal time constant. Based on the characteristic numbers a method is proposed to distinguish between pyrolysis at low and high heating rate conditions for biomass fuels used in state-of-the-art combustion plants. By these means, the application ranges of low and high heating rate TGA experiments are clearly determined.

2. Particle model

In order to investigate the effect of the boundary conditions on the heating rate in a biomass particle during pyrolysis, an in-house code for modelling thermal conversion of thermally thick particles was used. The layer model accounts for intra-particle transport processes and simultaneous sub-processes of thermal conversion of thermally thick solid biomass particles. To reduce the model complexities and calculation time, only the radial temperature gradient in the particle is considered. This is an usual simplification assumption. Its validity was already addressed by Ha and Choi [14].

To apply the one-dimensional model for a finite cylindrical geometry (as an approximation for the biomass particle shape), Thunman's discretisation [3] approach has been applied. This approach assumes that the particle boundary conditions are homogeneous and every point in the particle at a certain distance from the particle surface has the same temperature and conversion state. The particle is divided into four layers: drying layer, pyrolysis layer, char and ash layer. The boundaries between the layers are related to the conversion sub-processes: drying, pyrolysis and char burnout fronts. At the beginning of the thermal conversion process only drying is of relevance. Due to heating up, moisture starts to get released from the particle. The pyrolysis layer consists of dry biomass and is located around the drying layer as the drying front moves towards the particle centre. When pyrolysis commences, the dry biomass converts to char and volatiles. Volatiles leave the particle and char builds a layer around the pyrolysis layer. Finally, char burnout also creates another layer which contains only ash and surrounds the char layer. As the conversion of the fuel particle proceeds, drying, pyrolysis and char burnout fronts move from the surface to the centre of the particle. Fig. 1 shows the scheme of the layer model for a cylindrical thermally thick particle at a certain time when all the sub-processes of thermal conversion are existing.

The conversion of each layer is simulated by separate submodels. It is assumed that drying occurs at a fixed boiling temperature in an infinitely thin zone that separates the wet and the dry part of the particle. Such a steep drying front for the fast drying of biomass is reported almost by all drying models [15]. The drying process acts as a heat sink, it means that any amount of heat flow above the boiling temperature is consumed by the drying process. This approach to calculate the evaporation rate is the most often used model in literature, for instance [4–6,16–20]. It is assumed that there is no resistance to mass transfer, and therefore the water vapour instantaneously leaves the particle. However, the cooling effect of the water vapour transfer through the particle is considered. Therefore the drying rate is controlled by heat transfer.

Biomass pyrolysis is described by decomposition of its three pseudo-components hemicellulose, cellulose, and lignin. This model implicitly assumes the hypothesis of an independent decomposion of these three constituents. An Arrhenius equation is used to describe the pyrolysis of each pseudo-component. It represents the dependence of the kinetic rate constant k on the absolute temperature T:

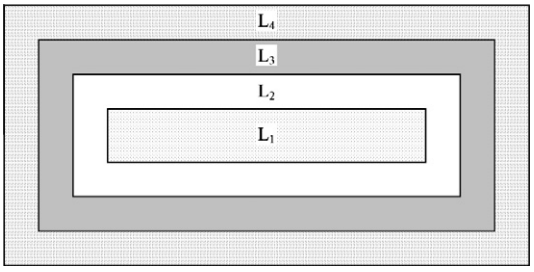

Fig. 1. Scheme of the layer model; L_1... drying layer; L_2... pyrolysis layer; L_3... char layer; L_4... ash layer.

$$k = A\exp\left(-\frac{E}{RT}\right) \tag{1}$$

A is the pre-exponential factor, E is the activation energy and R is the universal gas constant.

The overall mass loss rate of a particle during pyrolysis is given as:

$$-\frac{dm}{dt} = \sum_{i=1}^{3} c_i \frac{d\alpha_i}{dt} \tag{2}$$

where i is related to each pseudo-component, $c_i = m_{0,i} - m_{f,i}$ is a measure of the contribution of the partial decomposition processes to the overall mass loss $m_0 - m_f$. The conversion of each pseudo-component α_i can be expressed by:

$$\alpha_i = \frac{m_{0,i} - m_i}{m_{0,i} - m_{f,i}} \tag{3}$$

The pseudo-components are all assumed to decompose individually according to a first-order reaction, therefore the conversion rate of each pseudo-component is given by:

$$\frac{d\alpha_i}{dt} = A_i \exp\left(-\frac{E_i}{RT}\right)(1-\alpha_i) \tag{4}$$

Char conversion models are more complicated than biomass pyrolysis models, as they are based on heterogeneous reactions for which both intrinsic kinetic and transport phenomena are important. It has been experimentally verified that char combustion is such a rapid reaction that it occurs in a very thin layer [21]. Due to the structure of the layer model, the char conversion reactions are assumed to occur at the interface between char and ash layer. Char oxidation with O_2 and gasification with CO_2, H_2O and H_2 are considered as char conversion reactions. The heterogeneous reaction rate constants are listed in Table 1. The rate of char conversion reactions is a function of both kinetic rate at the reaction surface and mass transfer rate to/from the reaction surface. Assuming a global reaction rate of first order with respect to the oxidising/gasifying agent concentration at the reaction surface, leads to char conversion rate as:

$$\frac{dm_{ch}}{dt} = -\sum_{i=1}^{4} \frac{\Omega_i M_c}{\frac{1}{k_i S} + \frac{1}{h_m S} + \int_{\delta_{ash}} \frac{dr}{\mathcal{D}_e} S(r)} X_{\infty,i} \tag{5}$$

where $i = 1$–4 corresponds to the heterogeneous reactions in Table 1 and Ω_i is the stoichiometric ratio of moles of carbon per mole of oxidising/gasifying agent in the corresponding reaction. M_c, S, k_i, δ_{ash} and $X_{\infty,i}$ are the carbon molecular weight, the surface area of the char burnout front, the kinetic rate constant of heterogeneous reaction i, the thickness of the ash layer and the molar concentration of oxidising/gasifying agent of reaction i at the bulk flow, respectively.

The mass transfer coefficient of reactant species in the boundary layer around the particle h_m, is obtained by the Sherwood number. The effective diffusivity of the ash layer $\mathcal{D}_e$, depends on the ash porosity ϕ, the tortuosity η, and the molecular diffusivity of the penetrating gaseous component $\mathcal{D}_a$:

$$\mathcal{D}_e = \frac{\phi}{\eta}\mathcal{D}_a \tag{6}$$

Table 1
Heterogeneous reaction kinetic rate constants [22].

$\Omega C + O_2 \rightarrow 2(\Omega-1)CO + (2_\Omega)CO_2$	$k_c = 1.715\ T\ exp(-9000/T)$
	$\Omega = \frac{2[1+4.3\ exp(-3390/T)]}{2+4.3\ exp(-3390/T)}$
$C + CO_2 \rightarrow 2CO$	$k_c = 3.42\ T\ exp(-15{,}600/T)$
$C + H_2O \rightarrow CO + H_2$	$k_c = 3.42\ T\ exp(-15{,}600/T)$
$C + 2H_2 \rightarrow CH_4$	$k_c = 3.42 \times 10^{-3}\ T\ exp(-15{,}600/T)$

The tortuosity can be replaced by the inverse of the porosity, which is often a reasonable approximation [23–25]:

$$\mathcal{D}_e = \phi^2 \mathcal{D}_a \tag{7}$$

Since particle shrinkage during drying is much lower compared to that occurring during pyrolysis and charcoal combustion [26], it is postulated that during drying, the size of the particle remains constant and its density decreases. However, both shrinkage and density change during the pyrolysis and char burnout are considered in the layer model.

The external surface of the particle exchanges heat and mass with the surroundings. Boundary conditions are required to complete the system of equations. The symmetry boundary condition is applied for the energy equation, at the particle centre which leads to zero heat flux. The Neumann boundary condition is used at the particle surface with known emissivity, ϵ, and radiation, T_{rad}, as well as convection, T_{conv}, temperatures:

$$\lambda\left(\frac{\partial T}{\partial r}\right)_{r=R} = \epsilon\sigma\left(T_{rad}^4 - T_{r=R}^4\right) + h_{conv}(T_{conv} - T_{r=R}) \tag{8}$$

where σ is the Stefan–Boltzmann constant. h_{conv} is the convective heat transfer coefficient and is determined by an appropriate correlation for the Nusselt number. For spherical particles the Ranz–Marshall correlation and for cylindrical particles the correlation proposed by Churchill and Bernstein are applied [27].

To validate the layer model, experimental data of a single-particle reactor reported by Lu et al. [7] were utilised. Measured particle surface temperatures, centre temperatures and mass loss during thermal conversion of cylindrical particles under oxidising and non-oxidising conditions were compared with the predictions of the layer model. Table 2 summarises the physical and chemical properties used in the simulations of the single particle reactor. Some of the results of validation simulations are presented in Figs. 2 and 3. The model predictions for particle centre and surface temperature as well as the particle mass loss profile agree well with experiments. A detailed description of the layer model and its application for the simulation of an underfeed stoker furnace are presented in [9].

In this study the validated layer model is applied to calculate the heating rate in different biomass particles under various pyrolysis conditions.

3. Pyrolysis mass loss function

The mass loss rate of each pseudo-component, Eq. (4), for constant heating rate experiments $T = \beta t + T_0$, can be rearranged to:

$$\frac{d\alpha_i}{dT} = \frac{A_i}{\beta}\exp(1-\alpha_i) \tag{9}$$

If one looks for the temperature at which the maximum conversion rate of each pseudo-component occurs T_m, the second derivative of α_i in respect to temperature is required:

$$\frac{d^2\alpha_i}{dT^2} = \frac{A_i}{\beta}\exp\left(-\frac{E_i}{RT}\right)\left[\frac{E_i}{RT^2}(1-\alpha_i) - \frac{d\alpha_i}{dT}\right] \tag{10}$$

The extrema of the conversion rate of each pseudo-component are the roots of equation $d^2\alpha_i/dT^2 = 0$. Considering Eqs. (10) and (9) results in:

$$\frac{E_i}{RT} - \ln\left(\frac{RA_i}{E_i\beta}T^2\right) = 0 \tag{11}$$

Eq. (11) might have only one root. According to the DTG curves this root corresponds to the temperature T_m for each pseudo-component. This equation was also applied as a characteristic pyrolysis temperature by Saastamoinen [19].

Table 2
Parameters used in the simulations.

Proximate analysis (wt.% d.b.)				Ultimate analysis (wt.% d.b.)			
	Poplar	Spruce	Beech		Poplar	Spruce	Beech
C	48.1	52.04	48.3	Volatiles	90	81.2	78.1
H	5.77	6.07	6.0	Char	9.5	18.3	21.29
O	45.53	40.99	44.99	Ash	0.5	0.5	0.61
N	0.1	0.4	0.1				

	Density (kg m^{-3})	Conductivity [7] (W m^{-1} K^{-1})	Heat capacity [34] (J kg^{-1} K^{-1})
Dry wood	545[a] [7]	$0.14 + 6.5 \times 10^{-4}T$	$1500 + T$
Char	200 [28]	0.071	$420 + 2.09T + 6.85 \times 10^{-4}T^2$
Ash	300	1.2	$420 + 2.09T + 6.85 \times 10^{-4}T^2$
Water	998.2	0.6	4182
Particle emissivity (–)	$\epsilon = 0.85$		
Bulk flow velocity (m/s)	1		

	Hemicellulose	Cellulose	Lignin
Pyrolysis model [10]			
A (s^{-1})	2.527×10^{11}	1.379×10^{14}	2.202×10^{12}
E (kJ mol^{-1})	147	193	181
Char conversion model			
Pore diameter (μm)	100 [29]		
Porosity of ash layer	0.9		

[a] Poplar wood.

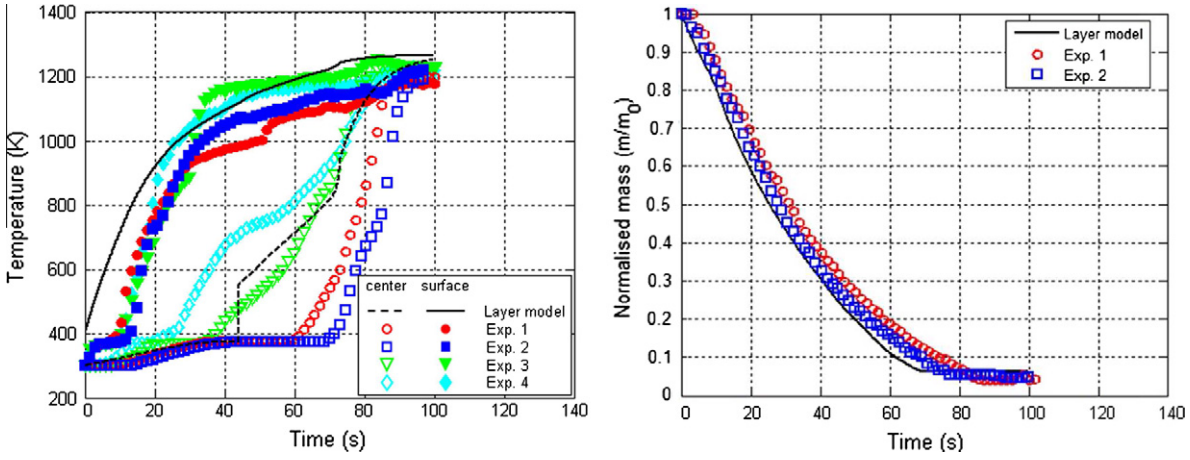

Fig. 2. Comparison between simulated and measured temperature and normalised mass profiles during pyrolysis of a cylindrical poplar wood particle; $D = 9.5$ mm, $L = 38$ mm, $MC = 40\%$ w.b. $T_{rad} = 1276$ K; the experimental data are from Lu et al. [7].

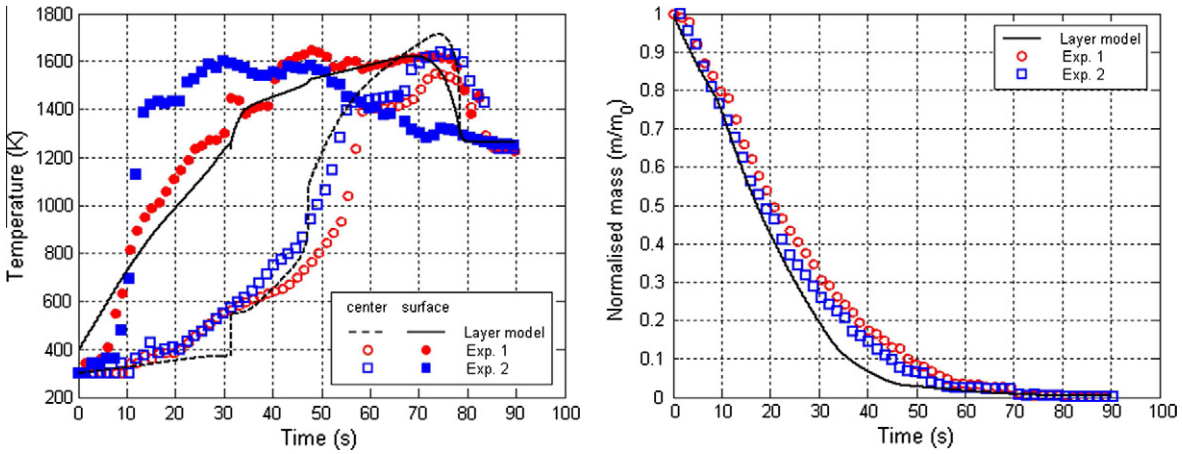

Fig. 3. Comparison between simulated and measured temperature and normalised mass profiles during combustion of a cylindrical poplar wood particle; $D = 9.5$ mm, $L = 9.5$ mm, $MC = 40\%$ w.b., $T_{rad} = 1276$ K; the experimental data are from Lu et al. [7].

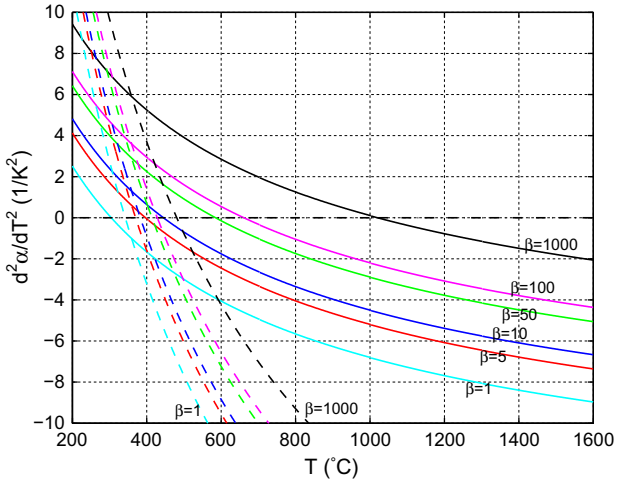

Fig. 4. Effect of the heating rate on the root of Eq. (11), β is given in (K/min). Solid lines are related to kinetic data obtained at 5 (K/min): $A = 3.98$ (1/s), $E = 46$ (kJ/mol) [30] and dashed lines are related to kinetic data obtained at 80 (K/min): $A = 2.202 \times 10^{12}$ (1/s), $E = 181$ (kJ/mol) [10].

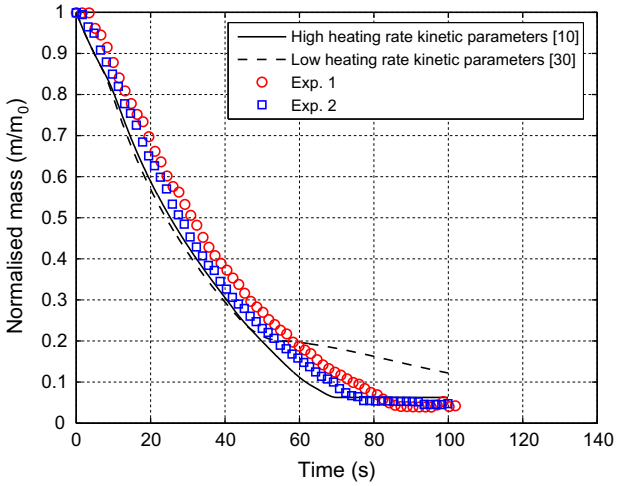

Fig. 5. Effect of applying high and low heating rate kinetic parameters for the simulation of pyrolysis of a poplar particle under high heating rate conditions; the pyrolysis conditions are the same as in Fig. 2; the experimental data are from Lu et al. [7].

Several experimental results [10–13,31–33] confirm that increasing the heating rate moves the DTG curves towards higher temperatures. This lateral shift or delayed decomposition might be attributed to the residence time of the sample. Since a higher heating rate means shorter exposure to a certain temperature or temperature domain, the sample needs to reach higher temperatures to have enough time for completion of the overall decomposition.

As it can be seen the second term of Eq. (11) is a function of the heating rate β. For a given set of kinetic parameters, i.e. A_i and E_i, any changes in the heating rate alert T_m and successively lead to a lateral shift of the DTG curve. In other words, as the heating rate increases, the DTG curves as well as the temperature T_m move towards higher temperatures. Fig. 4 illustrates the effect of the heating rate on the root of Eq. (11). In this figure the kinetic data for the decomposition of beech lignin at low and high heating rates (5 and 80 K/min) were applied [10,30]. The temperature T_m increases in both sets of kinetic data, when the heating rate raises from 1 to 1000 K/min.

Accordingly, the pyrolysis mass loss function is able to predict the lateral shift of DTG curves by changing the heating rate. However, applying low heating rate kinetic parameters overestimates the increase of T_m. It can be explained by the ratio of the pre-exponential factor to the activation energy. As it is seen in Eq. (11), if this ratio is small, the temperature for the maximum conversion rate drastically changes by variations of the heating rate. Almost in all TGA experiments at low heating rate the ratio of the pre-exponential factor to the activation energy is small enough to result in an unrealistic T_m, particularly for lignin.

Fig. 5 shows the effect of applying high and low heating rate kinetic parameters for the simulation of pyrolysis of a poplar particle under high heating rate conditions. As it can be seen the simulation results obtained by applying the high heating rate kinetic parameters are in agreement with the experimental data. At the end of pyrolysis (attributed to pyrolysis of lignin), there is a deviation between the simulation results obtained by applying the low heating rate kinetic parameters and the measured values. It indicates that applying the low heating rate kinetic parameters for the simulation of a high heating rate case leads to much slower mass loss rate during the pyrolysis of lignin in comparison to the measurements as well as the results of the simulation with the high heating rate kinetic parameters. It means that the pyrolysis of lignin in the case of applying the low heating rate kinetic parameters begins at higher temperatures. Hence, as it is shown in Fig. 4, the increase of T_m has been over-predicted by applying the low heating rate kinetic parameters.

Therefore, using kinetic parameters measured at low heating rate TGA experiments for the simulation of pyrolysis in high heating rate regime leads to an unrealistic shape of the DTG curves. It, successively, impairs the overall mass loss profile during pyrolysis.

4. Influencing parameters on the heating rate

The rate of variation of temperature distribution inside a biomass particle over time as it is exposed to an external heat flux, depends on the particle density ρ, specific heat capacity c_p, size, thermal conductivity λ_s as well as the heat flux itself. The moisture content also indirectly affects the heating rate. It changes the particle density, heat capacity and thermal conductivity. To generalise the investigation of the effects of these parameters on the heating rate, they are summarised in the Biot number and the thermal time constant:

$$Bi = \frac{h_e L_c}{\lambda_s} \tag{12}$$

$$\tau = \frac{\rho_s c_p L_c}{h_e} \tag{13}$$

where h_e is the effective heat transfer coefficient and L_c is the particle characteristic length which is the ratio of the particle volume to its surface area. Such a definition for the characteristic length facilitates its calculation for particles with various shapes. The effective heat transfer coefficient can be defined as:

$$h_e = h_{rad} + h_{conv} = \epsilon\sigma(1 + \theta + \theta^2 + \theta^3)T_{rad}^3 + \frac{\lambda_g Nu}{L_c} \tag{14}$$

where $\theta = \frac{T_p}{T_{rad}}$.

The Biot number gives a measure of the ratio between the heat transfer resistances inside and at the surface of the particle. The thermal time constant shows the respond of the particle to changes in its thermal environment. In other words, a big thermal time constant means that the particle temperature changes slowly over time.

Since the particle size and physical properties as well as the external heat flux change during the thermal conversion of a particle, the Biot number and thermal time constant of a particle depend on the degree of conversion. However, one can consider a certain state of the particle conversion and calculate these two characteristic numbers based on the reference state. Therefore, in this study, the Biot number and thermal time constant based on the initial condition are used to classify the particle pyrolysis conditions. Additionally, for calculating the effective heat transfer coefficient (Eq. (14)), the physical properties of air at the corresponding radiation temperature are used. The Ranz–Marshall correlation is applied for the Nusselt number.

5. Results and discussion

The layer model simulation results of the pyrolysis of a spruce pellet with 8% w.b. moisture content, 6 mm diameter and 3 cm length which is exposed to 700 °C radiation temperature in an oxidising environment, are presented in Fig. 6. The particle surface temperature and the temperature at the centre of the pyrolysis layer at the beginning are the same and they increase with different slopes. Due to the drying process the boundary between the drying layer and the pyrolysis layer moves towards the particle centre. Therefore, the thickness of the pyrolysis layer increases which results in a deviation of the pyrolysis layer centre temperature from the particle surface temperature. When the char burnout starts (after about 25 s), the particle surface temperature sharply increases which results in a big deviation from the pyrolysis layer centre temperature. Approaching the end of pyrolysis, this difference declines because the pyrolysis layer thickness decreases as a result of dry wood decomposition. At the end of the pyrolysis process the pyrolysis layer vanishes and the char and ash layer remain.

Since pyrolysis happens in the pyrolysis layer, the time derivative of its centre temperature is an indicator for the heating rate at which pyrolysis takes place. The time derivative of the pyrolysis layer centre temperature is presented in Fig. 7. Moreover, the released volatiles over time, expressed as percentage of the total amount of the volatiles is shown in Fig. 7. It can be seen that at the beginning the heating rate dramatically decreases from a large value to about 340 K/min and it remains constant for some seconds. There is a local minimum at time about 15 s. It is due to the end of the drying process. The end of drying means that the drying layer disappears which results in some numerical instabilities in the layer model.

The heating rate of the pyrolysis layer is directly proportional to the temperature difference between the surface temperature and the pyrolysis layer centre temperature, the thermal conductivity and the inverse of the distance between the particle surface and the centre of the pyrolysis layer. As it is shown in Fig. 6, the fast increase of the particle surface temperature at the beginning of char burnout results in a large difference between the surface temperature and the temperature at the centre of the pyrolysis layer. Therefore, the heating rate of the pyrolysis layer increases between 25 and 30 s.

Afterwards, the increasing rate of the particle surface temperature declines and stays constant. At the same time, the pyrolysis layer centre temperature gradually increases. Hence, the difference between this temperature and the particle surface temperature declines. Additionally, conversion of dry wood to charcoal during pyrolysis decreases the thermal conductivity, because the conductivity of charcoal is less than that of dry wood [34]. Therefore, the heating rate gradually decreases between 30 and 55 s. Then, it raises, because the distance between the particle surface and the centre of the pyrolysis layer rapidly declines. The rate of decrease

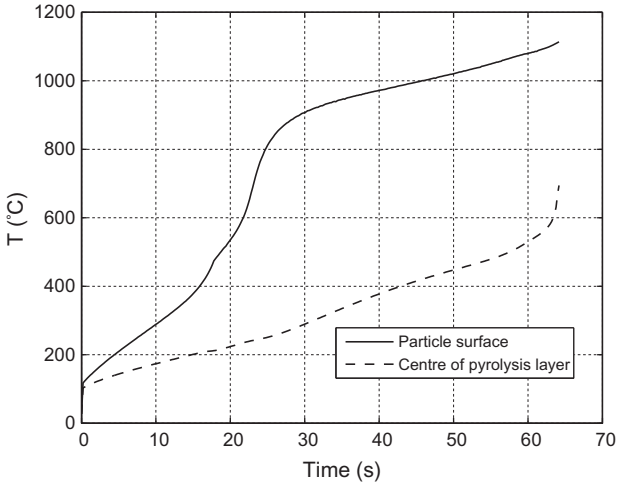

Fig. 6. Simulated temperatures of the particle surface and of the centre of the pyrolysis layer for a spruce pellet with $D = 6$ mm, $L = 30$ mm and $MC = 8\%$ w.b. exposed to $T_{rad} = 700$ °C during pyrolysis in an oxidising environment.

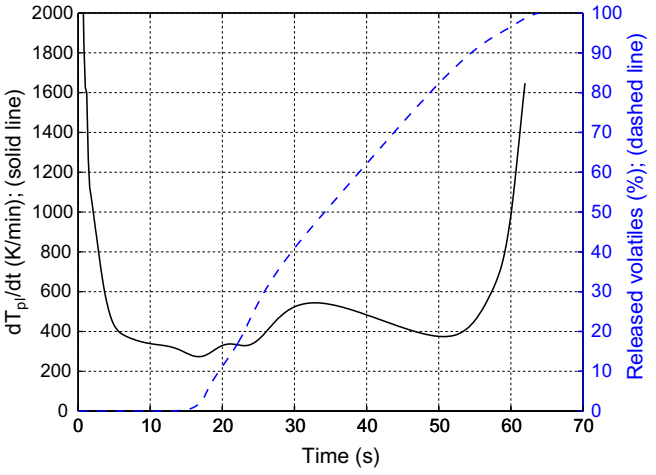

Fig. 7. Time derivative of the centre temperature of the pyrolysis layer presented in Fig. 6 and percentage of volatiles released during the pyrolysis of the spruce pellet.

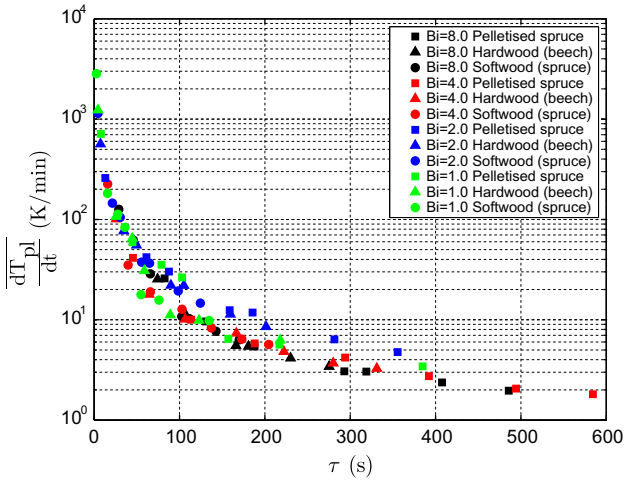

Fig. 8. Volatiles release rate weighted average of the heating rate of the pyrolysis layer vs. thermal time constant for various Biot numbers and different biomass fuels (data according to Table 3).

Table 3
Average of the heating rate of the pyrolysis layer centre temperature weighted by pyrolysis rate in dependence of the Biot number, the thermal time constant and biomass particle density as presented in Fig. 8.

Case	T (°C)	MC (%w.b.)	D (m)	L (m)	Pelletised spruce ρ_p = 1200 (kg/m^3)		Hardwood (beech) ρ_p = 680 (kg/m^3)		Softwood (spruce) ρ_p = 420 (kg/m^3)	
					τ (s)	$\overline{\frac{dT_{pl}}{dt}}$ (K/min)	τ (s)	$\overline{\frac{dT_{pl}}{dt}}$ (K/min)	τ (s)	$\overline{\frac{dT_{pl}}{dt}}$ (K/min)
Bi = 8.0										
1	1326	8	0.050	0.080	82.65	25.86	46.83	60.51	28.93	1.26e^2
2	1192	8	0.060	0.120	1.31e^2	9.63	74.37	25.46	45.93	62.21
3	1100	8	0.070	0.100	1.88e^2	5.42	1.07e^2	11.47	65.8	28.74
4	1004	10	0.085	0.210	2.93e^2	3.06	1.66e^2	5.52	1.03e^2	10.77
5	982	10	0.084	0.300	3.19e^2	3.04	1.81e^2	5.43	1.12e^2	10.24
6	923	10	0.093	0.400	4.08e^2	2.37	2.30e^2	4.15	1.43e^2	7.68
7	880	10	0.100	0.500	4.86e^2	1.96	2.75e^2	3.42	1.70e^2	6.31
Bi = 4.0										
1	1214	8	0.025	0.050	45.53	41.42	25.80	1.01e^2	15.93	2.25e^2
2	998	10	0.040	0.070	1.14e^2	10.03	64.43	17.91	39.80	35.07
3	872	10	0.050	0.100	1.88e^2	5.81	1.07e^2	10.11	65.85	18.95
4	845	20	0.055	0.145	2.94e^2	4.20	1.67e^2	7.34	1.03e^2	12.70
5	777	20	0.065	0.150	3.92e^2	2.74	2.22e^2	4.82	1.37e^2	8.31
6	801	30	0.070	0.130	4.94e^2	2.06	2.80e^2	3.70	1.73e^2	6.41
7	762	30	0.075	0.150	5.84e^2	1.81	3.31e^2	3.27	2.05e^2	5.67
Bi = 2.0										
1	1206	8	0.009	0.024	13.08	2.59e^2	7.41	5.66e^2	4.58	1.14e^3
2	832	8	0.019	0.060	61.23	42.03	34.70	76.96	21.43	1.45e^2
3	737	8	0.022	0.090	87.59	30.24	49.64	55.43	30.66	1.05e^2
4	710	20	0.030	0.060	1.59e^2	12.44	89.97	22.06	55.57	37.48
5	672	20	0.031	0.080	1.86e^2	11.80	1.05e^2	22.00	64.96	36.58
6	577	20	0.040	0.080	2.81e^2	6.37	1.60e^2	11.36	98.52	19.35
7	527	20	0.045	0.090	3.56e^2	4.76	2.02e^2	8.53	1.24e^2	14.63
Bi = 1.0										
1	900	8	0.005	0.013	7.90	7.11e^2	4.56	1.24e^3	2.76	2.84e^3
2	477	8	0.012	0.030	45.05	59.22	25.75	1.07e^2	15.77	1.82e^2
3	467	20	0.015	0.030	78.89	35.32	44.70	64.88	27.61	1.13e^2
4	510	30	0.016	0.035	1.03e^2	26.43	58.79	30.83	36.07	83.46
5	397	30	0.020	0.035	1.57e^2	6.44	89.15	11.17	55.06	17.81
6	427	40	0.020	0.050	2.17e^2	5.65	1.23e^2	9.88	75.98	15.71
7	387	50	0.025	0.050	3.85e^2	3.43	2.18e^2	6.25	1.35e^2	9.83

of pyrolysis layer thickness at the end of pyrolysis is significantly higher than at the beginning of pyrolysis, because of the gradual increase in pyrolysis layer temperature during pyrolysis and the fact that the pyrolysis rate is an exponential function of temperature.

The main outcome of Fig. 7 is that the heating rate during the release of volatiles varies between 300 and more than 1000 K/min for the spruce pellet under the given conditions. However, most of the volatiles are released at heating rates between 300 and 550 K/min. It shows that in order to define a value which is an appropriate indicator for the heating rate during pyrolysis both the heating rate and the release rate of volatiles at that heating rate have to be considered. Therefore, the volatiles release rate weighted average of the heating rate is introduced as:

$$\overline{\frac{dT_{pl}}{dt}} = \frac{\sum_{i=1}^{n}\left(\frac{dT_{pl}}{dt}\right)_i \cdot \left(\frac{dm_{vol}}{dt}\right)_i}{\sum_{i=1}^{n}\left(\frac{dm_{vol}}{dt}\right)_i} \tag{15}$$

where i is related to each time step during the pyrolysis. $\overline{\frac{dT_{pl}}{dt}}$ for Fig. 7 is 461 K/min.

The volatiles release rate weighted average of the heating rate of the pyrolysis layer versus the thermal time constant for different Biot numbers and biomass fuels are presented in Fig. 8. For each Biot number several cases with various radiation temperatures, moisture contents and particle sizes were taken into account (they can be seen in Table 3 and by the markers in Fig. 8). Since the Biot number is independent of density, for each Biot number three different particle densities, 420, 680 and 1200 kg/m^3 are considered for softwood (spruce), hardwood (beech) and pelletised spruce, respectively. The physical properties used in Eqs. (12) and (13) are reported in Table 2. As already mentioned the Biot number and the thermal time constant are calculated based on the initial condition. Therefore, the physical properties are related to the moist fuel and the effect of the moisture content is considered by using the mass weighted mixing law:

$$X_{moistfuel} = (1 - MC)X_{dryfuel} + MCX_{water} \tag{16}$$

where X denotes the physical properties, e.g. density, specific heat and thermal conductivity and MC is the fuel moisture content.

An increase in density at a constant Biot number increases the thermal time constant which can be simply explained by Eq. (13). The comparison between different biomass fuels (densities) for a certain case indicates that the heating rate decreases by an increase in density, because the particles with higher density need more thermal energy for a certain change in their temperature over time.

According to Fig. 8, the heating rate exponentially declines by increasing the thermal time constant. This can be explained by the definition of the thermal time constant, i.e. the tendency of the particle to retain its temperature while its thermal environment has been changed. The variation of the Biot number has only a negligible effect on the heating rate in comparison to the variation of thermal time constant.

In addition, since each Biot number can result in both high and low heating rate regimes between 1000 K/min and less than 10 K/

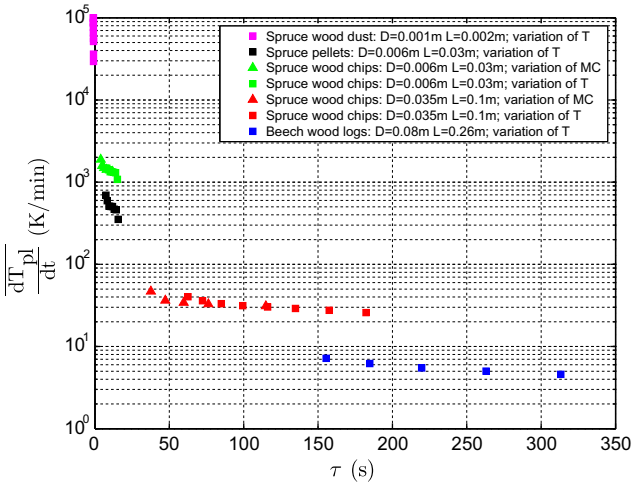

Fig. 9. Volatiles release rate weighted average of the heating rate of the pyrolysis layer vs. thermal time constant for different biomass fuels used in state-of-the-art combustion plants (data according to Table 4).

min, the Biot number cannot be used to specify the heating rate regime during pyrolysis. However, the thermal time constant can determine the heating rate regime. As it can be seen in Fig. 8, the cases with thermal time constants higher than 50 s indicate a low heating rate regime, i.e. $\frac{dT_{pl}}{dt} < 50$ K/min.

Additionally, the pyrolysis rate weighted average of the heating rate of different biomass fuels applied in state-of-the-art combustion/gasification plants versus the thermal time constant are shown in Fig. 9. Pellets, wood chips, wood dust and wood logs have been chosen to cover most biomass combustion applications. Pellets according to the Austrian standard (ÖNORM M7135) typically show a moisture content of 8% w.b. as well as a diameter of 0.006 m and a length of 0.03 m. Regarding wood chips two different sizes were considered, one particle size class similar to pellets (small wood chips) and another one with a diameter of 0.035 m and a length of $L = 0.1$ m (large wood chips). The moisture content of wood chips has been varied between 10 and 55% w.b. Additionally, wood logs according to the Austrian standard (ÖNORM CEN/TS 14961) with a moisture content of 12% w.b. (M20), a diameter of 0.08 m and a length of 0.26 m (P250) have been considered. Since the layer model is applicable for cylindrical and spherical shapes, the wood log is assumed to be cylindrical. The diameter and length of an equivalent cylindrical wood log were calculated by keeping the volume and surface area constant. Wood dust was considered to be cylindrical with a moisture content of 10% w.b., a diameter of 0.001 m and a length of 0.002 m.

Pellets, wood logs and wood dust typically show a rather constant moisture content, therefore, only the effect of radiation temperature on the heating rate was investigated for these biomass fuels. However, for wood chips the effects of both radiation temperature and moisture content were examined, due to the possible big variations in moisture contents. Radiation temperature varied between 600 and 1300 °C for all biomass types, except for wood dust, where radiation temperatures up to 1500 °C have been considered. In Table 4 the corresponding data shown in Fig. 9 are listed. By these variations concerning biomass type and combustion conditions all typical applications like stoves, fixed and fluidised bed combustion/gasification systems as well as dust combustion plants are considered.

Fig. 9 indicates that wood dust and wood pellet pyrolysis always occur in high heating rate regimes. On the other hand wood log pyrolysis happens in a low heating rate regime. For wood chips the heating rate regime depends on the particle size. The effect of density can also be seen in Fig. 9 by comparison between spruce pellets and spruce wood chips of the same size. The higher the density the lower the heating rate (in agreement with the results of Fig. 8). A comparison between the effects of moisture content and radiation temperature on the heating rates of wood chips shows that radiation temperature has a bigger influence, particularly for small wood chips. It can be stated that moisture content does not strongly influence the heating rate regime of a certain biomass particles.

Table 4
Biot number, thermal time constant and heating rate of different biomass fuels as presented in Fig. 9 in dependence of radiation temperature and moisture content.

T (°C)	Spruce wood dust D = 0.001 m, L = 0.002 m				Spruce pellets D = 0.006 m, L = 0.03 m				Beech wood logs D = 0.08 m, L = 0.26 m			
	MC (%w.b.)	Bi (–)	τ (s)	$\frac{dT_{pl}}{dt}$ (K/min)	MC (%w.b.)	Bi (–)	τ (s)	$\frac{dT_{pl}}{dt}$ (K/min)	MC (%w.b.)	Bi (–)	τ (s)	$\frac{dT_{pl}}{dt}$ (K/min)
600	10	0.49	0.21	2.83e^4	8	0.87	15.61	3.53e^2	12	3.55	3.13e^2	4.58
700	10	0.52	0.20	3.48e^4	8	0.95	14.29	4.61e^2	12	4.23	2.62e^2	5.02
800	10	0.56	2.71	4.96e^4	8	1.05	12.95	4.68e^2	12	5.06	2.19e^2	5.48
900	10	0.59	0.19	5.41e^4	8	1.15	11.81	5.04e^2	12	6.02	1.85e^2	6.21
1000	10	0.64	0.18	6.30e^4	8	1.28	10.61	5.07e^2	12	7.16	1.55e^2	7.18
1100	10	0.70	0.16	7.40e^4	8	1.43	9.45	5.10e^2	–	–	–	–
1200	10	0.78	0.15	8.27e^4	8	1.64	8.28	5.95e^2	–	–	–	–
1300	10	0.84	0.14	8.51e^4	8	1.83	7.42	6.93e^2	–	–	–	–
1400	10	0.90	0.13	9.58e^4	–	–	–	–	–	–	–	–
1500	10	0.96	0.11	9.61e^4	–	–	–	–	–	–	–	–
	Spruce wood chips D = 0.006 m, L = 0.03 m				Spruce wood chips D = 0.035 m, L = 0.1 m							
1000	10	1.26	3.89	1.89e^3	10	3.88	37.64	46.89				
1000	20	1.17	4.88	1.58e^3	20	3.61	47.30	36.31				
1000	30	1.10	6.16	1.49e^3	30	3.38	59.71	34.25				
1000	40	1.03	7.87	1.42e^3	40	3.18	76.26	32.86				
1000	55	0.95	11.86	1.34e^3	55	2.91	1.15^2	31.01				
600	50	0.66	51.10	1.08e^3	50	1.64	1.82e^2	25.87				
700	50	0.72	13.83	1.30e^3	50	1.89	1.58e^2	27.56				
800	50	0.80	12.54	1.32e^3	50	2.21	1.35e^2	29.01				
900	50	0.87	11.42	1.34e^3	50	2.57	1.16e^2	30.27				
1000	50	0.97	10.27	1.34e^3	50	3.00	99.43	31.42				
1100	50	1.09	9.14	1.42e^3	50	3.51	85.01	33.20				
1200	50	1.25	8.01	1.47e^3	50	4.12	72.36	36.07				
1300	50	1.39	7.18	1.48e^3	50	4.77	62.54	40.41				

6. Summary and conclusions

The influence of the heating rate on the pyrolysis kinetic model and successively on the overall mass loss of biomass particles, raises the demand to investigate the range of heating rates which may occur during pyrolysis. For this purpose a one-dimensional single particle model was utilised to simulate the temperature profile inside biomass particles as well as the particles mass loss during pyrolysis under various conditions. The average of the time derivative of the pyrolysis layer centre temperature weighted by the volatiles release rate was found to be an appropriate indicator for the heating rate in biomass particles during pyrolysis.

It was shown that the heating rate is mainly affected by the radiation temperature and the particle size. Moreover, the density of the biomass particles has a relevant influence. Compared to the other parameters, the moisture content shows only small influences. The influencing parameters on the heating rate were summarised in the Biot number and the thermal time constant, in order to generalise the investigations. It has been found that the heating rate exponentially decreases as the thermal time constant increases. The variation of the Biot number has only a negligible effect on the heating rate. Therefore, to specify the heating rate regime the thermal time constant is sufficient. The results show that if the thermal time constant is more than 50 s, pyrolysis happens in a low heating rate regime, i.e. $\frac{dT_{pl}}{dt} < 50$ K/min.

Additionally, the heating rate during pyrolysis of different biomass fuels applied in state-of-the-art combustion plants was examined. A broad range of biomass types and thermal conversion conditions were considered to cover all typical biomass combustion applications. It was found that pyrolysis of wood dust and wood pellets always occur in high heating rate regimes. Furthermore, wood log pyrolysis always takes place in a low heating rate regime. However, the heating rate regime during pyrolysis of wood chips is dependent on the particle size.

The results clearly show for which biomass fuels and combustion conditions the results of conventional TGA systems (typically with heating rates well bellow 50 K/min) can be applied and when kinetic parameters derived from high heating rate experiments are needed. This distinguishment is of great importance, because at present in many cases pyrolysis kinetic parameters derived from low heating rate TGA experiments are incorrectly used.

References

[1] Peters B. Measurements and application of a discrete particle model (DPM) to simulate combustion of a packed bed of individual fuel particles. Combust Flame 2002;131:132–46.

[2] Wurzenberger JC, Wallner S, Raupenstrauch H, Khinast JG. Thermal conversion of biomass: comprehensive reactor and particle modeling. AIChE J 2002;48:2398–410.

[3] Thunman H, Leckner B, Niklasson F, Johnsson F. Combustion of wood particles – a particle model for Eulerian calculations. Combust Flame 2002;129:30–46.

[4] Bruch C, Peters B, Nussbaumer T. Modelling wood combustion under fixed bed conditions. Fuel 2003;82:729–38.

[5] Porteiro J, Miguez JL, Granada E, Morán JC. Mathematical modelling of the combustion of a single wood particle. Fuel Process Technol 2006;87:169–75.

[6] Porteiro J, Granada E, Collazo J, Patiño D, Morán JC. A model for the combustion of large particles of densified wood. Energy Fuels 2007;21:3151–9.

[7] Lu H, Robert W, Peirce G, Ripa B, Baxter LL. Comprehensive study of biomass particle combustion. Energy Fuels 2008;22:2826–39.

[8] Lu H, Ip E, Scott J, Foster P, Vickers M, Baxter LL. Effects of particle shape and size on devolatilization of biomass particle. Fuel 2010;89:1156–68.

[9] Mehrabian R, Stangl S, Scharler R, Obernberger I. CFD simulation of biomass grate furnaces with a comprehensive 3D packed bed model. In: 25th German flame day conference, Karlsruhe, Germany; September 2011.

[10] Branca C, Albano A, Di Blasi C. Critical evaluation of wood devolatilization mechanisms. Thermochim Acta 2005;429:133–41.

[11] Antal MJ, Várhegyi G. Cellulose pyrolysis kinetics: the current state of knowledge. Ind Eng Chem Res 1995;34:703–17.

[12] Várhegyi G, Antal MJ, Jakab E, Szabo P. Kinetic modeling of biomass pyrolysis. J Anal Appl Pyrol 1996;42:73–8.

[13] Teng H, Wei YC. Thermogravimetric studies on the kinetics of rice hull pyrolysis and the influence of water treatment. Ind Eng Chem Res 1998;37:3806–11.

[14] Ha MY, Choi BR. A numerical study on the combustion of a single carbon particle entrained in a steady flow. Combust Flame 1994;97:1–16.

[15] Di Blasi C. Multi-phase moisture transfer in the high-temperature drying of wood particles. Chem Eng Sci 1998;53:353–66.

[16] Galgano A, Di Blasi C. Modeling the propagation of drying and decomposition fronts in wood. Combust Flame 2004;139:16–27.

[17] Yang YB, Sharifi VN, Swithenbank J, Ma L, Darvell LI, Jones JM, et al. Combustion of a single particle of biomass. Energy Fuels 2008;22:306–16.

[18] Thunman H, Davidsson K, Leckner B. Separation of drying and devolatilization during conversion of solid fuels. Combust Flame 2004;137:242–50.

[19] Saastamoinen JJ. Simplified model for calculation of devolatilization in fluidized beds. Fuel 2006;85:2388–95.

[20] Bilbao R, Mastral JF, Lana JA, Ceamanos J, Aldea ME, Betrán M. A model for the prediction of the thermal degradation and ignition of wood under constant and variable heat flux. J Anal Appl Pyrol 2002;62:63–82.

[21] Gómez-Barea A, Leckner B. Modelling of biomass gasification in fluidized bed. Prog Energy Combust Sci 2010;36:444–509.

[22] Johansson R, Thunman H, Leckner B. Influence of intraparticle gradients in modeling of fixed bed combustion. Combust Flame 2007;149:49–62.

[23] Froment GF, Bischoff KB. Chemical reactor analysis and design. New York: John Wiley & Sons; 1990.

[24] Johnson MFL, Stewart WE. Pore structure and gaseous diffusion in solid catalysts. J Catal 1965;4:248–52.

[25] Patisson F, Francois MG, Ablitzer D. A non-isothermal, non-equimolar transient kinetic model for gas–solid reactions. Chem Eng Sci 1998;53:97–708.

[26] Kumar RR, Kolar AK, Leckner B. Shrinkage characteristics of Casuarina wood during devolatilization in a fluidized bed combustor. Biomass Bioenergy 2006;30:153–65.

[27] Incropera FP, De Witt DP. Introduction to heat transfer. 2nd ed. New York: John Wiley & Sons; 1990.

[28] Bergström D, Israelsson S, Öhman M, Dahlqvist S, Gref R, Boman C, et al. Effects of raw material particle size distribution on the characteristics of Scots pine sawdust fuel pellets. Fuel Process Technol 2008;89:1324–9.

[29] Sreekanth M, Sudhakar DR, Prasad BVSSS, Kolar AK, Leckner B. Modelling and experimental investigation of devolatilizing wood in a fluidized bed combustor. Fuel 2008;87:2698–712.

[30] Grønli MG, Várhegyi G, Di Blasi C. Thermogravimetric analysis and devolatilization kinetics of wood. Ind Eng Chem Res 2002;41:4201–8.

[31] Williams PT, Besler S. The influence of temperature and heating rate on the slow pyrolysis of biomass. Renew Energy 1996;7:233–50.

[32] Biagini E, Fantei A, Tognotti L. Effect of the heating rate on the devolatilization of biomass residues. Thermochim Acta 2008;472:55–63.

[33] Mani T, Murugan P, Abedi J, Mahinpey N. Pyrolysis of wheat straw in a thermogravimetric analyzer: effect of particle size and heating rate on devolatilization and estimation of global kinetics. Chem Eng Res Des 2010;88:952–8.

[34] Grønli M. A theoretical and experimental study of the thermal degredation of biomass. PhD thesis, Norway: The Norwegian University of Science and Technology; 1996.